5. References

1. K.R. Nary, R. Nubling, S. Becccue, W.T. Colleran, J. Penny, K-C Wang, "An 8-bit, 2 giga-sample per second analog to digital converter", in Tech. Dig. GaAS IC 17th Annual Symp. 1995, pp. 303.
2. P.E. Pace, D. Styer, "High-resolution encoding process for an integrated optical analog-to-digital converter", J. Opt. Eng. Vol 33 (8), pp. 2638, 1994.
3. H.F. Taylor, "An optical analog-to-digital converter—design and analysis", IEEE Jour. Quantum Elect., Vol. QE-15, pp. 210, 1974.

CTuM40 **1:00 pm**

1.55 μm DFB laser integrated on Erbium doped phosphate glass substrate

S. Blaize, J.E. Broquin, D. Barbier,* C. Cassagnètes,* *LEMO-ENSERG, UMR 5530, INPG-UJF-CNRS, BP 257, 38016 Grenoble, France,* Email: blaize@enserg.fr; broquin@enserg.fr; *Teem-Photonics 61 chemin du vieux Chêne, 38240 Meylan, France*

The development of Wavelength Division Multiplexing (WDM) telecommunications systems has driven the rapid development of Erbium doped fiber amplifier and very narrow band lasers.[1] Recently, new efficient waveguide amplifier on phosphate glass has been demonstrated.[2] In this paper, we present the first steps of fabrication and analysis of 10 monolithically integrated DFB lasers on a chip. The starting point of our work is an Er/Yb co-doped phosphate glass, on which buried channel waveguides have been realized using ion exchanged techniques.[2] Recent progress in that technology has led to a gain of 3dB/cm. The waveguides present a mean index variation of 2.10^{-2} above substrate refractive index value of 1.52. For operation at 1.55 μm, the grating period predicted by the Bragg phase matching condition is $d = \lambda/2n_e = 0.505$ μm related to the mean effective index n_e of the waveguides. In this work, a corrugate 1 cm long grating was made on the top of the wafer. Interferometric exposure of photoresist with an Ar^+1 aser operating at 488 nm was used to print the grating. After development, the grating pattern is transferred on the glass surface through a Reactive Ion Etching process. The glass is etched sufficiently to get more than 60% of reflectivity at Bragg wavelength. Under pumping at 980 nm, single longitudinal mode operation around 1.55 μm is demonstrated for all the ten waveguides of the chip.

Figure 1 shows the narrow emission line measured with a 0.1 nm resolution Optical Spectrum Analyser. On the inset we show the line observed with a 15 GHz free spectral range Fabry Perot analyser, the FWHM exhibited here is less than 130 MHz which is the nominal resolution of the resonator. On figure 2, a near field pattern of the laser output intensity is shown. Finally, power characterisation of the micro-laser n°5 on the chip is displayed on figure 3. The maximum power emission is 0.8 mW for 75 mW of pump power. Threshold is 25 mW and the slope efficiency is 1.6%. Further promising investigations in the technological process will allow a better feedback efficiency and therefore decrease lasing threshold and increase the slope efficiency.

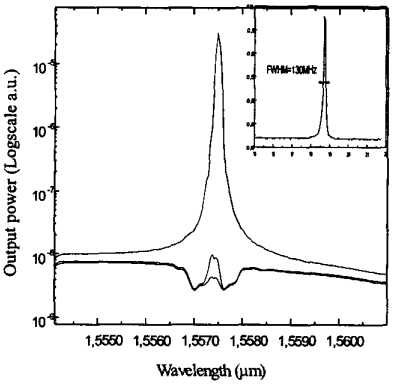

CTuM40 Fig. 1. Transmitted power spectrum with Optical Spectrum Analyser and Fabry-Pérot.

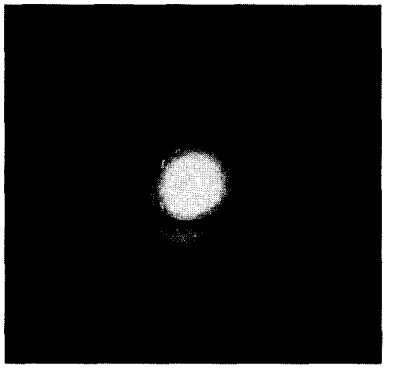

CTuM40 Fig. 2. Near field pattern of the laser output.

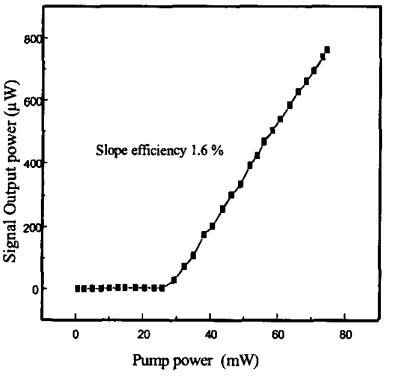

CTuM40 Fig. 3. Transmitted Power at 1,55 μm versus Pumping power at 980 nm.

1. W.H. Loh, B.N. Samson, L. Dong, G.J. Cowle, and K. Hsu, Journal of Lightwave Technology, Vol 16, No 1, 1998.
2. D. Barbier, M. Rattay, F. Saint-André, A. Kevorkian, J.-M.P. Delavaux, and E. Murphy, presented at the ECOC'96, Oslo, Norway, paper WeD2.2.

CTuM41 **1:00 pm**

Light propagation and localization in randomly spaced gratings in a single mode fiber

Baruch Fischer and Ofer Shapira, *Department of Electrical Engineering, Technion-Israel Institute of Technology Haifa 32000, Israel; Email: fischer@ee.technion.ac.il*

Wave propagation in random media has attracted much attention throughout the years, where optics and quantum mechanics were the natural ground for these activities. One of the most important finding was the Anderson localization effect, originally studied for electrons in disordered solids.[1] Thereafter, many works were done in the field.

Here we present a study of light propagation in a randomly spaced fiber grating system, showing localization properties. The transmittance decay, has an exponential dependence on the number of gratings, in accordance with the localization theory. The interesting feature is that the result contradicts the naive ray theory assumption that the random phases, associated with the randomly varying spacing between the gratings make the system incoherent. Then one would expect a $T_N \propto T/N$ dependence for the N gratings intensity transmittance, where T is the single grating transmittance. The study here, along the known results of the localization theory, shows that the decay is exponential, $T_N = exp[-Nlog(1/7)]$, and the multiple internal reflections between the different gratings tend to cancel in the transmittance due to destructive interference.[2] The result can be of interest for uses of long random grating arrays, as well as for the study of localization in ideal 1-dimensional systems.

Wave propagation in 1-dimensional random media was previously examined in many works. Examples are works with light and acoustic waves.[2,3] The physical basis of localization in disordered systems is similar. The diffusion coefficient vanishes because of the coherent interference between waves scattered from random scatterers. Mathematically, it is possible to describe the propagation by a product of transfer matrices. The asymptotic behavior of such a product is given by Furstenberg's theorem[4] on products of random matrices. It ensures that under very general conditions, the elements of the matrix product and any norm of it, grow exponentially with the same exponent.

The subject of this paper is the propagation of light in a fiber with random refractive index scatterers formed by successive fiber gratings separated by random spacings. We have carried out a detailed analysis of the system, by defining the suitable transfer matrix for a set of successive fiber gratings. In our case the spacings between two successive gratings vary over several wavelengths, and therefore we could evaluate the inverse localization length in the strong disordered regime.

In the experiment, we tested the transmitted

CTuM41 Fig. 1. The random fiber grating system.

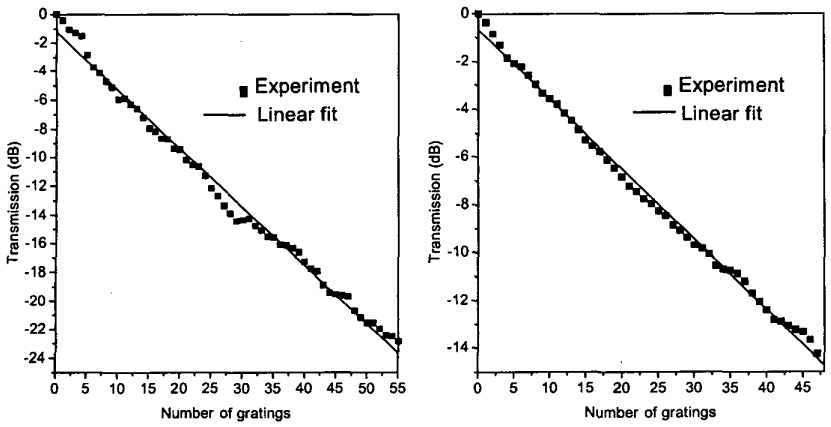

CTuM41 Fig. 2. Two sets of measurements for the grating number dependence N of the light transmittance.

intensity through a sequence of randomly spaced gratings (Fig. 1). The light source was the spontaneous emission from an erbium doped fiber amplifier. The transmitted light was measured after every fabrication of an additional grating in the array. The gratings were made by the known method of UV light illumination of the fiber through a phase mask. In our case, all gratings had the same Bragg wavelength, with approximately the same reflectivity and spectral width. The typical grating length was about 1 *mm*. The spacing between the gratings was arbitrary in the range of 0.5 *mm* to 1.5 *mm*, ensuring a uniform distribution over a wavelength scale. The relevant wavelength region for our study is the central reflectivity band of the gratings.

A multiple fiber grating system behaves as an interferometric system, and thus is very sensitive to temperature fluctuations, changes in the fiber tension and acoustic noise. To avoid these problems during the experiment, all the measurements carried out included averaging over 0.5 nm at the middle of the grating spectral reflectivity band. The justification for that is that the asymptotic property of a long string of matrices is approximated by averages over short strings.

We show in Fig. 2, experimental data for two sets of measurements for different fiber gratings. We see that the transmittance decays exponentially, as predicted from the wave theory. Also the decay exponents (inverse localization length) fit the theoretical expression given above, where the single grating transmittance T is taken from the experiment. It is obtained by a direct measurement of the transmittance of the first two gratings, regarded as Fabry-Perot etalons. The obtained values for T were –0.41dB for Fig. 2(a) and –0.30dB for Fig. 2(b).

References

1. P.W. Anderson, Phys. Rev. **109**, 1492 (1958).
2. Berry, M.V. and Klein, S. (1997) *Eur. J. Phys.* **18** 222–228.
3. Baluni, V. and Willemsen, J. (1985) *Phys. Rev. A* **31** 3358–3363.
4. Furstenberg, H. (1963) *Trans. Am. Math. Soc.* **108** 377–428.

CTuM42 **1:00 pm**

In-line Fiber Optic Comb Filter Using a Polished $LiNbo_3$ Overlay Waveguide for a Multi-wavelength Source

Kyung-Rak Sohn, Jong-Hoon Lee, D.I. Seo, and Jae-Won Song, *Department of Electronics Engineering, Kyungpook National University, Taegu, 702-701, Korea; Email: krsohn99@palgong.knu.ac.kr*

Wavelength-division multiplexing (WDM) is one of the key solutions for providing greater bandwidth in optical communication networks. Recently, multi-layer dielectric filters, silica waveguides or diffraction gratings have been used to fabricate the WDM devices.[1] Especially, a multi-wavelength erbium-doped fiber ring lasers by using a comb filter have been reported.[2–4] In this paper, we firstly demonstrated a side-polished fiber-optic comb filter and propose the application as a channel isolation filter for a WDM-based multi-wavelength light source.

The demonstrated comb filter is composed of a side-polished single mode fiber with a polished 200 μm-$LiNbO_3$a s multi-mode overlay waveguide (MMOW) as shown in Fig. 1. The single mode optical fiber fixed in the V-groove is glued by NOA65. A 200 μm-MMOW made by polishing of the $LiNbO_3$ are attached on. The space of between the fiber block and MMOW is filled with NOA61, which also plays the role of the buffer layer enhancing the coupling efficiency and reducing the optical losses at the interaction region. The evanescent field coupling from the polished region of the fiber to the polished $LiNbO_3$ layer can explain the comb filtering characteristics.[5–6] When a particular mode of MMOW is phase matched with a fiber mode, strong directional coupling has been occurred. The number of coupled mode is dependent on the thickness and the refractive index of MMOW and decided the comb spacing. Narrower comb spacing can be obtained from the higher refractive index and thicker MMOW. We have used a cover glass, polymers and a polished $LiNbO_3$ as a MMOW. Fig. 2 (a) shows the transmission spectrum of a side-polished fiber optic comb filter by the 200 μm $LiNbO_3$ overlay waveguide in 200 nm band over 1400 nm–1600 nm. Because of the birefringence of $LiNbO_3$, the comb filter is only passed the TM mode in the measured wavelength range. The comb spacing is about 4nm and insertion loss is 7dB under the 2 nm resolution in 40 nm wavelength band as shown in Fig. 2 (b). Relatively large insertion loss has been caused by the thickness of MMOW and the refractive index difference with fiber core. We expect that the refractive index control of the buffer layer reduce the insertion loss.

In conclusion, in-line fiber optical comb filters using a polished $LiNbO_3$ overlay waveguide have been demonstrated. The proposed comb filter can be applied to the channel isolation filter of the multi-wavelength light source having the wide spectral range of the fiber optic communications.

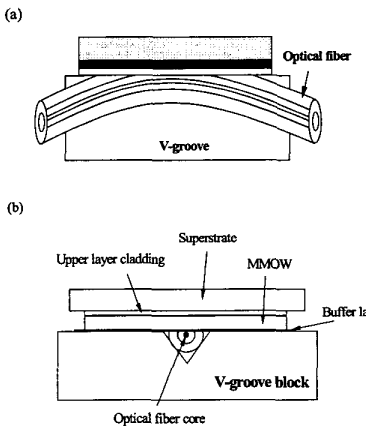

CTuM42 Fig. 1. Schematic diagram of in-line fiber optic comb filter with a polished $LiNbO_3$. (a) Side view. (b) Front view.

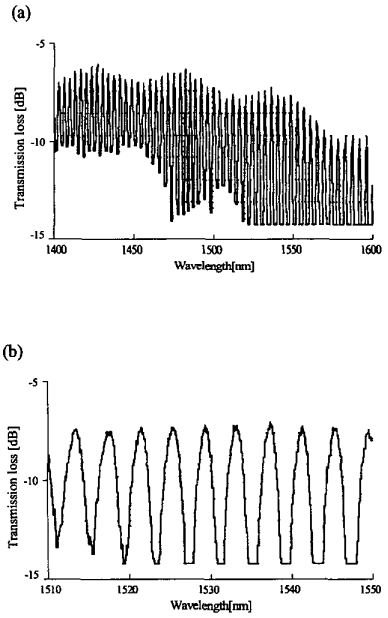

CTuM42 Fig. 2. Transmission spectra of in-line fiber optic comb filter. The light is a TM mode. (a) Resonance peaks in a 200 nm band. (b) 4 nm comb spacing in 1.5 μm wavelength range.